Targeting glutaminase is therapeutically effective in ibrutinib-resistant mantle cell lymphoma

Lingzhi Li,[1] Lei Nie,[1] Alexa Jordan,[1] Qingsong Cai,[1] Yang Liu,[1] Yijing Li,[1] Yuxuan Che,[1] Jovanny Vargas,[1] Zhihong Chen,[1] Angela Leeming,[1] Wei Wang,[1] Yixin Yao,[1] Michael Wang[1,2] and Vivian Changying Jiang[1]

[1]Department of Lymphoma and Myeloma and [2]Department of Stem Cell Transplantation and Cellular Therapy, The University of Texas MD Anderson Cancer Center, Houston, TX, USA

Correspondence: V.C. Jiang
cjiang@mdanderson.org

Received: June 6, 2022.
Accepted: November 10, 2022.
Early view: November 24, 2022.

https://doi.org/10.3324/haematol.2022.281538

Abstract

Mantle cell lymphoma (MCL) is an incurable B-cell non-Hodgkin lymphoma characterized by frequent relapses. The development of resistance to ibrutinib therapy remains a major challenge in MCL. We previously showed that glutaminolysis is associated with resistance to ibrutinib. In this study, we confirmed that glutaminase (GLS), the first enzyme in glutaminolysis, is overexpressed in ibrutinib-resistant MCL cells, and that its expression correlates well with elevated glutamine dependency and glutaminolysis. Furthermore, we discovered that GLS expression correlates with MYC expression and the functioning of the glutamine transporter ASCT2. Depletion of glutamine or GLS significantly reduced cell growth, while GLS overexpression enhanced glutamine dependency and ibrutinib resistance. Consistent with this, GLS inhibition by its specific inhibitor telaglenastat suppressed MCL cell growth both *in vitro* and *in vivo*. Moreover, telaglenastat showed anti-MCL synergy when combined with ibrutinib or venetoclax *in vitro*, which was confirmed using an MCL patient-derived xenograft model. Our study provides the first evidence that targeting GLS with telaglenastat, alone or in combination with ibrutinib or venetoclax, is a promising strategy to overcome ibrutinib resistance in MCL.

Introduction

Mantle cell lymphoma (MCL) is highly refractory to clinical treatments and very frequently relapses, which has created a great demand for more effective therapy.[1] For example, ibrutinib is a potent inhibitor of Bruton tyrosine kinase (BTK) with proven efficacy in the treatment of MCL,[2] but nearly all initially responsive patients eventually develop ibrutinib resistance. Our group has recently shown that ibrutinib-resistant MCL cells exhibit increased glutaminolysis, the process of glutamine metabolism contributing to the tricarboxylic acid cycle.[3] This suggests that glutaminolysis could be targeted as a potential therapeutic strategy to overcome ibrutinib resistance.

The rapid growth of cancer cells requires a fast metabolic rate and large energy supply, so cellular metabolic processes, especially glycolysis and glutaminolysis, are often dysregulated.[4] Glycolysis is preferentially used for fuel in many types of cancer (the Warburg effect), generating a sufficient ATP supply to support cancer cell growth while using less oxygen than the canonical Krebs cycle.[5] However, there is increasing evidence that glutaminolysis is the main source of ATP supply in some other types of cancer, including MCL[3] and multiple myeloma.[6] Glutamine is first transported from the extracellular space to the cytosol and then to mitochondria for glutaminolysis.[7] The first step of glutaminolysis is catalysis of glutamine to glutamate, which is performed by the glutaminase (GLS) enzymes coded by two paralogous genes: *GLS* on chromosome 2 and *GLS2* on chromosome 12.[8] We previously showed that overexpression of GLS, but not GLS2, is associated with ibrutinib resistance in MCL.[3] This suggests that GLS is potentially vulnerable for targeting of glutaminolysis to overcome ibrutinib resistance in MCL.

In this study, we confirmed that GLS expression is increased in multiple ibrutinib-resistant cell lines and primary patients' samples. We investigated the role of glutamine dependency and GLS overexpression in ibrutinib-resistant MCL cells. Furthermore, we evaluated the preclinical efficacy of targeting GLS either alone or in

combination with BTK or BCL2 inhibitors to overcome therapeutic resistance *in vivo* and *in vitro*.

Methods

Patients and collection of their samples

Fresh surgical biopsies and peripheral blood specimens were collected from patients after provision of informed consent and approval by the Institutional Review Board at the MD Anderson Cancer Center. Ficoll-Hypaque density centrifugation was used to isolate mononuclear cells as previously reported.[9] The patients' characteristics are summarized in *Online Supplementary Table S1*.

Cell culture and reagents

The MCL cell lines JeKo-1, Rec-1, Mino, Maver-1, and Z138 were obtained from the American Type Culture Collection. JeKo-1, Rec-1, and Mino are ibrutinib-sensitive cell lines, while Maver-1 and Z138 cell lines show primarily resistance to ibrutinib. The ibrutinib-resistant JeKo-R and JeKo-BTK-KD cell lines were established as previously described.[10] Briefly, JeKo-R cells were established from JeKo-1 cells by exposing these latter to stepwise dose increases of ibrutinib, while JeKo-BTK KD cells were genetically edited by CRISPR-Cas9 technology to have one allele of the *BTK* gene knocked out, resulting in dramatically reduced expression of BTK. The MCL cells were cultured in a 5% CO_2 incubator at 37°C. Telaglenastat (A14396) was purchased from Adooq Biosciences; ibrutinib (S2680) and venetoclax (S8048) were purchased from Selleck Chemicals; V-9302 (HY-112683) was purchased from MCE/Fisher.

Cell viability, apoptosis and cell cycle assay

Cell viability, apoptosis and cell cycle assays were performed as described previously by Zhang *et al.*[11]

Western blot analysis

Western blots were performed as described previously.[10] The antibody against GLS was purchased from Abcam (Cat. # AB156876) and the antibody against β-actin was purchased from Sigma (A1978-200UL); all the other antibodies were purchased from Cell Signaling Technology (GAPDH, Cat. # 5174s; MYC, Cat. # 9402s; ASCT2, Cat. # 8057s; cyclin D1, Cat. # 2922s; CDK4, Cat. # 12790s; cyclin B1, Cat. # 4138s; ERK, Cat. # 12950s; cleaved PARP, Cat. # 5625S; and cleaved caspase 3, Cat. # 9661s).

Mitochondrial membrane potential and ATP production assays

Assays of mitochondrial membrane potential and ATP production were performed as described previously.[3]

Lentiviral packaging and lentiviral transduction for gene knockdown or overexpression

Lentiviral packaging and lentiviral transduction for gene knockdown or overexpression of genes were performed as described previously by Jiang *et al.*[12]

Mantle cell lymphoma cell line-derived xenograft or patient-derived xenograft mouse models

All experimental procedures and protocols were approved by the Institutional Animal Care and Use Committee of The University of Texas MD Anderson Cancer Center. Drug evaluation, using cell line-derived xenograft (CDX) or patient-derived xenograft (PDX) mouse models, was performed as described previously.[11] Briefly, CDX and PDX tumors were established in mice that were treated orally twice daily with 100 mg/kg telaglenastat or daily with 50 mg/kg ibrutinib, 10 mg/kg venetoclax, or vehicle, until the maximum diameter of the tumor reached 15 mm. Tumor size was measured weekly, and tumor volume (in mm^3) was calculated as 0.5 × length × $width^2$. Tail blood was collected biweekly, and serum β_2-microglobulin level was measured according to the manufacturer's protocol.[11] The percentage of tumor cells ($CD20^+CD5^+$) in each tumor was determined by flow cytometry.

Gene set enrichment analysis and correlation with gene expression and patient survival.

These analyses were performed as described previously.[11] Briefly, alignment and read counting of the RNA-sequencing data were performed using STAR 2-pass alignment (v2.7.8a)[13] with the parameter quantMode as GeneCounts. Reads overlapping with the exons of each gene in the STAR ReadsPerGene.out.tab were determined. The batch effect was corrected using R package sva and differentially expressed genes were identified by DESeq2 (v1.32.0).[14] The enriched signaling pathways were determined by DESeq2 and gene set enrichment analysis (GSEA)[15] against the curated gene sets C2 from MSigDB.[15,16] Pathways related to glutamate metabolism were selected for further analysis. The GSEA pathway signature score was generated by the package TBSignatureProfiler with the gene list of interested pathways. Kaplan-Meier survival curves were analyzed with package survival.[17]

Statistical analysis

All statistical analyses were performed using GraphPad Prism. Data are represented as mean ± standard error of mean. An unpaired Student *t* test was used for comparisons between two groups. One-way or two-way analysis of variance was performed for comparisons of two or more groups. *P* values <0.05, 0.01, 0.001, and 0.0001 are flagged with *, **, *** and ****, respectively. *In vitro* experiments were performed at least twice, and each sample was tested in technical replicates.

Results

Ibrutinib-resistant mantle cell lymphoma cells overexpress glutaminase and are metabolically dependent on glutamine

Our previous study revealed that glutaminolysis is upregulated in ibrutinib-resistant MCL cells.[3] To validate this, we compared glutaminolysis signaling pathways in ibrutinib-resistant *versus* ibrubtinib-sensitive patients. Multiple signaling pathways involved in glutaminolysis were increased in ibrutinib-resistant patients (n=35) compared to ibrutinib-sensitive patients (n=35) (Figure 1A). Importantly, GLS expression correlated with glutaminolysis, including glutathione synthesis and recycling pathways (R=0.27, *P*=0.025) (Figure 1B). These data demonstrate the clinical significance of glutaminolysis and GLS overexpression in contributing to ibrutinib resistance. To further validate GLS overexpression in ibrutinib-resistant cells, we checked GLS protein expression by re-visiting our previous reverse phase protein array dataset.[3] GLS protein was confirmed to be overexpressed in ibrutinib-resistant cells (Z138 and Maver-1) compared to ibrutinib-sensitive cells (Rec-1 and Mino) (Figure 1C). This was further validated in additional MCL cell lines (n=5, *P*=0.0405) and primary patients' samples (n=6, *P*=0.0047) by western blotting (*Online Supplementary Figure S1A, B*). Based on

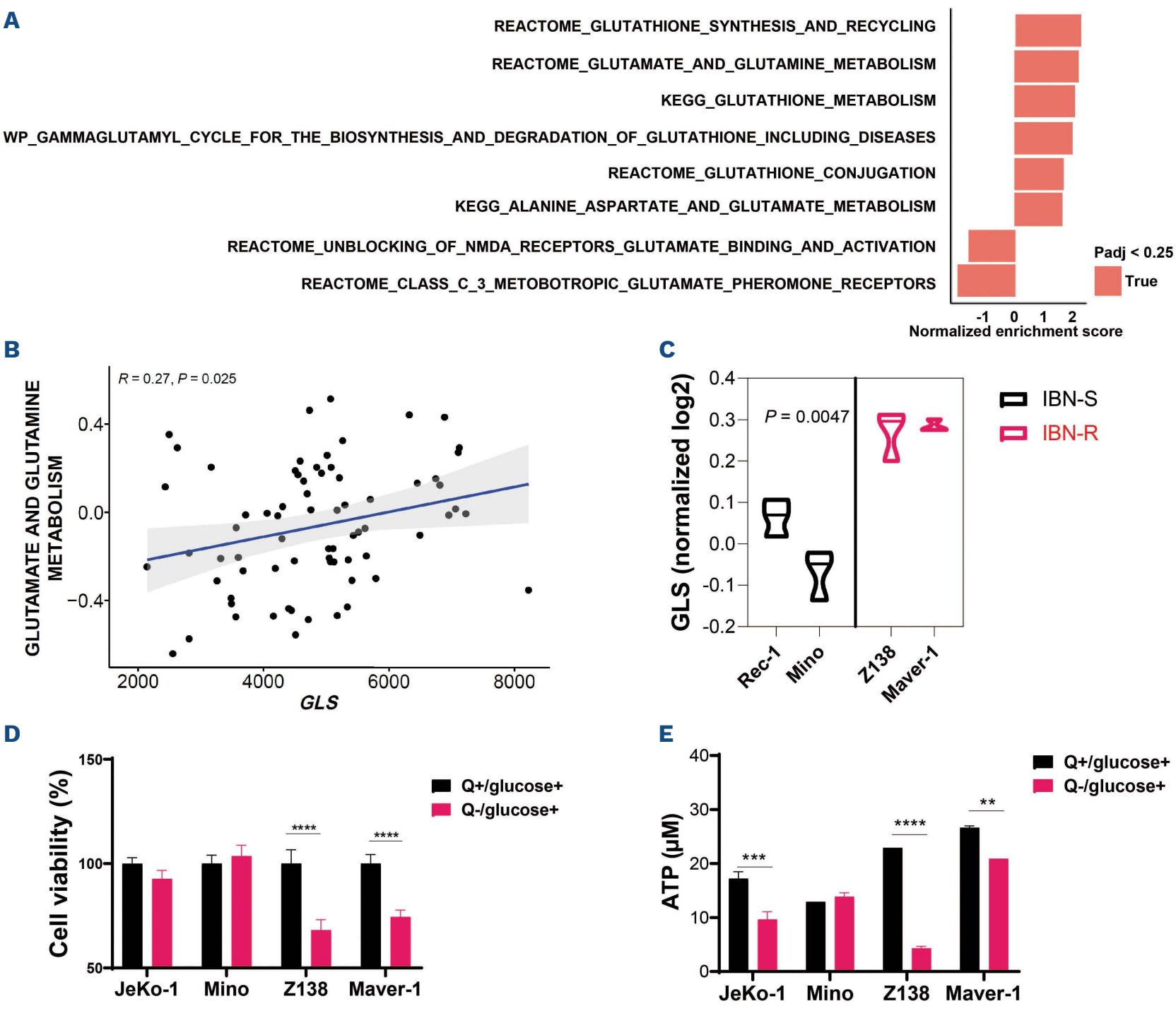

Figure 1. Ibrutinib-resistant mantle cell lymphoma cells overexpress glutaminase and are dependent on glutaminolysis. (A) Hallmark pathways from gene set enrichment analysis of bulk RNA-sequencing datasets were analyzed in ibrutinib-resistant (IBN-R) patients' samples (n=35) compared with ibrutinib-sensitive (IBN-S) patients' samples (n=35). (B) Pearson correlation of the glutamate and glutamine metabolic pathways with glutaminase (GLS) expression in patients' samples. (C) Reverse phase protein array in IBN-S and IBN-R cell lines as indicated. (D, E) IBN-S cell lines (JeKo-1 and Mino) and IBN-R cell lines (Z138 and Maver-1) were cultured in medium with (Q-/glucose+) or without (Q+/glucose+) depletion of glutamine (Q) for 24 h. Cell viability (D) and ATP production (E) were determined. The results are represented as mean ± standard deviation. An unpaired Student *t* test was used to determine statistical significance. **P*<0.05; ***P*<0.01; ****P*<0.001; *****P*< 0.0001.

these observations, we hypothesized that the survival and growth of ibrutinib-resistant MCL cells are dependent on glutaminolysis and glutamine supply. To test this, we depleted glutamine from the culture medium. Ibrutinib-resistant Z138 and Maver-1 cells, but not ibrutinib-sensitive Rec-1 and Mino cells, showed cell growth defects when glutamine was depleted (Figure 1D). Correspondingly, ATP production was greatly reduced by glutamine depletion (Figure 1E). Taken together, these data demonstrate that ibrutinib-resistant MCL cells overexpress GLS, the first enzyme in the process of glutaminolysis, and are metabolically dependent on the glutamine supply.

The glutamine transporter ASCT2 is required for ibrutinib resistance-associated glutamine dependency

To be used for glutamate synthesis in mitochondria, extracellular glutamine must be transported into the cytosol and then into the mitochondria. The transport into the cytosol relies on glutamine uptake mediated by the glutamine transporter ASCT2. We therefore examined ASCT2 expression in patients' samples. In the same cohort of patients as in Figure 1A-C, ASCT2 expression correlated well with glutathione synthesis and recycling pathways in ibrutinib-resistant MCL cells (R=0.61, P=1.4x10^{-8}) (Figure 2A) and with poor outcomes (P=0.019) (Figure 2B). Therefore, ASCT2 expression correlates with glutamine dependency in ibrutinib-resistant MCL cells.

To address whether there is any correlation between ASCT2 and GLS, we treated MCL cells with V-9302, an ASCT2-specific inhibitor, to block glutamine uptake. ASCT2 inhibition reduced GLS expression in JeKo-R and Z138 cells that normally express high levels of GLS (Figure 2C). To further address this, we knocked down GLS in Z138 cells using two independent short hairpin (sh)RNA (Figure 2D). Again, ASCT2 inhibitor treatment dramatically reduced the expression of GLS in Z138 with shCtrl, but no further reduction was observed in Z138 with shGLS#1 or shGLS#4. These data demonstrate that GLS expression

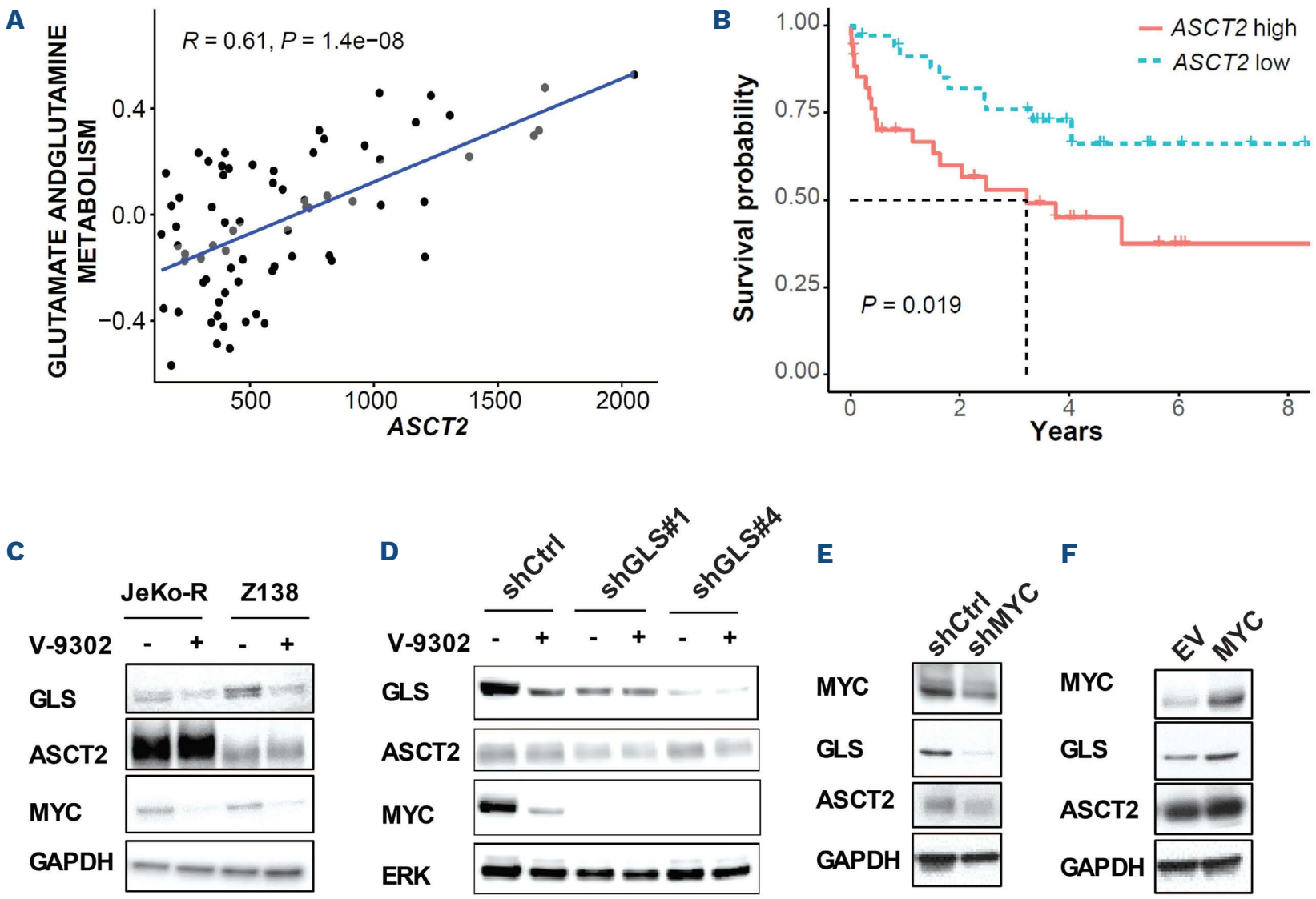

Figure 2. Glutaminase expression is regulated by the MYC-ASCT2 axis. (A) Pearson correlation of the glutamate and glutamine metabolic pathways with ASCT2 expression in samples from patients with mantle cell lymphoma (MCL), using the same cohort of patients as that in Figure 1A, B. (B) Kaplan-Meier survival curve plotted for patients' outcome based on ASCT2 expression using the same cohort of patients as that in Figure 1A, B. (C) JeKo-1 and Z138 cells were treated with 20 μM V-9302 (an ASCT2 inhibitor) for 48 h and harvested for immunoblotting with the indicated antibodies. (D) Z138 cells stably transduced with shCtrl, shGLS#1, or shGLS#4 were treated with 20 μM V-9302 for 8 h and harvested for immunoblotting with the indicated antibodies. (E) JeKo-1 cells stably transduced with shMYC or the corresponding control vector (shCtrl) were subjected to immunoblotting with the indicated antibodies. (F) Z138 cells were transduced with a control empty vector (EV) or MYC overexpression (MYC) were subjected to immunoblotting with the indicated antibodies. *P<0.05; **P<0.01; ***P<0.001; ****P<0.0001.

was sensitive to the blockage of glutamine uptake. ASCT2 is a MYC target[18] and MYC promotes GLS transcription through targeting of miR-23;[19] therefore, MYC is likely to be the master regulator of ASCT2-GLS-mediated glutaminolysis. To test this hypothesis, we knocked down MYC expression by shRNA in JeKo-1 cells. When MYC expression was low, GLS expression was barely detectable (Figure 2E). Meanwhile, when MYC was overexpressed in Z138 cells, GLS expression was upregulated (Figure 2F). These data suggest a positive feedback loop of MYC-ASCT2-GLS-mediated glutaminolysis: MYC promotes the expression of ASCT2 and GLS, and ASCT2-GLS-mediated glutaminolysis in turn leads to upregulated MYC expression.

Glutaminase is crucial for glutamine dependency in ibrutinib-resistant mantle cell lymphoma cells

To understand the role of GLS in contributing to glutamine dependency and ibrutinib resistance, we generated MCL cells with stable GLS overexpression from ibrutinib-sensitive JeKo-1 and Rec-1 cells (Figure 3A, *Online Supplementary Figure S2A*). We observed increased ibrutinib resistance in both cell lines engineered to overexpress GLS (Figure 3B, *Online Supplementary Figure S2B*). These GLS-overexpressing cells also showed enhanced dependency on glutamine for cell growth (Figure 3C, *Online Supplementary Figure S2C*). To investigate this further, we knocked down GLS expression in ibrutinib-resistant JeKo-R and Z138 cells (Figure 3D, *Online Supplementary Figure S2D*) with two independent shRNA. When GLS was knocked down, these cells became more sensitive to ibrutinib treatment (Figure 3E, *Online Supplementary Figure S2E*) and more dependent on glucose (Figure 3F, *Online Supplementary Figure S2F*). Taken together, these data demonstrated that GLS was crucial for glutamine dependency in ibrutinib-resistant MCL cells, and its overexpression contributed to ibrutinib resistance.

Glutaminase-mediated glutamine dependency promotes cell proliferation and ATP production in ibrutinib-resistant cells

To study the mechanism underlying cellular dependence

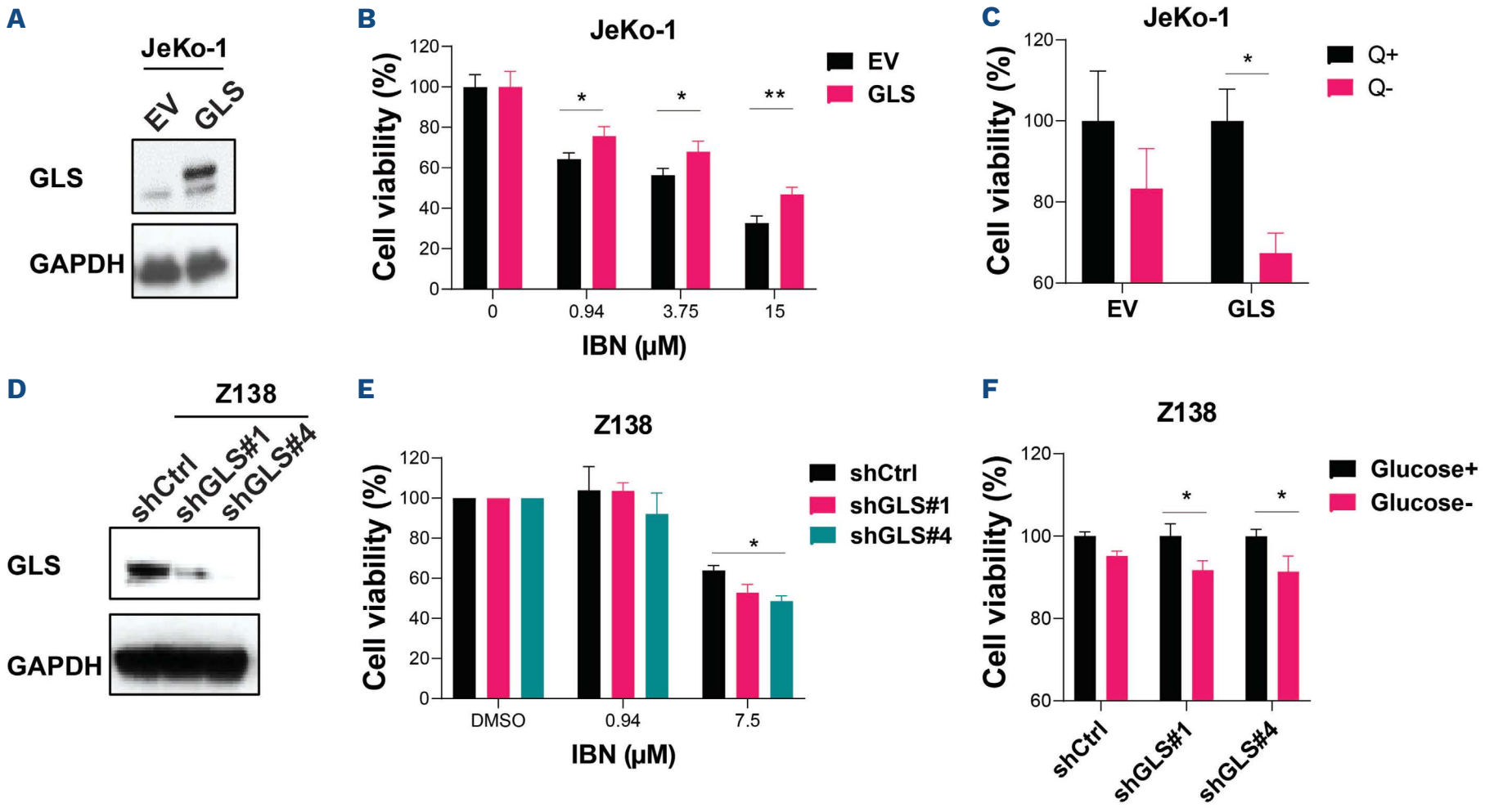

Figure 3. Glutaminase expression affects cell proliferation and ibrutinib sensitivity of mantle cell lymphoma cell lines. (A) JeKo-1 cells with or without stable glutaminase (GLS) overexpression (JeKo-1 EV and JeKo GLS, respectively) were harvested for immunoblotting with the indicated antibodies. (B) JeKo-1 EV and JeKo-1 GLS cells were treated with ibrutinib for 72 h at the indicated concentrations and cell viability was determined and plotted. (C) JeKo-1 EV and JeKo GLS cells were seeded for 24 h in culture medium with or without depletion of glutamine (Q) and cell viability was determined. (D) Z138 cells with or without stable GLS knockdown by shRNA (Z138-shCtrl, -shGLS#1, and -shGLS#4) were harvested for immunoblotting with the indicated antibodies. (E) Z138-shCtrl, -shGLS#1 and -shGLS#4 cells were treated with ibrutinib for 72 h at the indicated concentrations and cell viability was determined and plotted. (F) Z138-shCtrl, -shGLS#1 and -shGLS#4 cells were seeded for 24 h in culture medium with or without depletion of glucose and cell viability was determined. Two-way analysis of variance was used to determine statistical significance. ns: not significant; *P<0.05; **P<0.01; ***P<0.001; ****P<0.0001; IBN: ibrutinib; Q: glutamine; EV: empty vector; GLS: glutaminase.

on GLS-mediated glutamine metabolism, we examined GLS expression by depleting either glutamine or glucose in the culture medium. GLS expression was diminished by glutamine depletion but not glucose depletion in ibrutinib-resistant Z138 cells with control shRNA. Interestingly, cyclin D1 showed a similar expression pattern to GLS in these cells upon glutamine depletion (Figure 4A). Consistent with this, expression of cyclin D1 and GLS was higher in cells with acquired resistance to ibrutinib (JeKo-IBN-R) or venetoclax (Rec-Ven-R and Mino-Ven-R) compared to parental cells (*Online Supplementary Figure S3A*). Furthermore, expression of Ki-67, as a proliferation marker, and MYC was also higher in these resistant cells. This suggests that the MYC-GLS axis may promote cell cycle progression and cell proliferation. Indeed, cell proliferation was significantly reduced in ibrutinib-resistant Z138 and JeKo-R cells when GLS expression was depleted by shGLS#4 (Figure 4B, *Online Supplementary Figure S3B*). Z138-shGLS#4 consequently became more sensitive to glucose depletion (Figure 4C, D).

The maintenance of mitochondrial membrane potential is essential for cell proliferation.[20] Glycolysis is important for maintaining mitochondrial membrane potential and glutaminolysis associates with increased mitochondrial potential.[21] Both glutamine and glucose depletion in culture medium triggered a loss in mitochondrial potential in

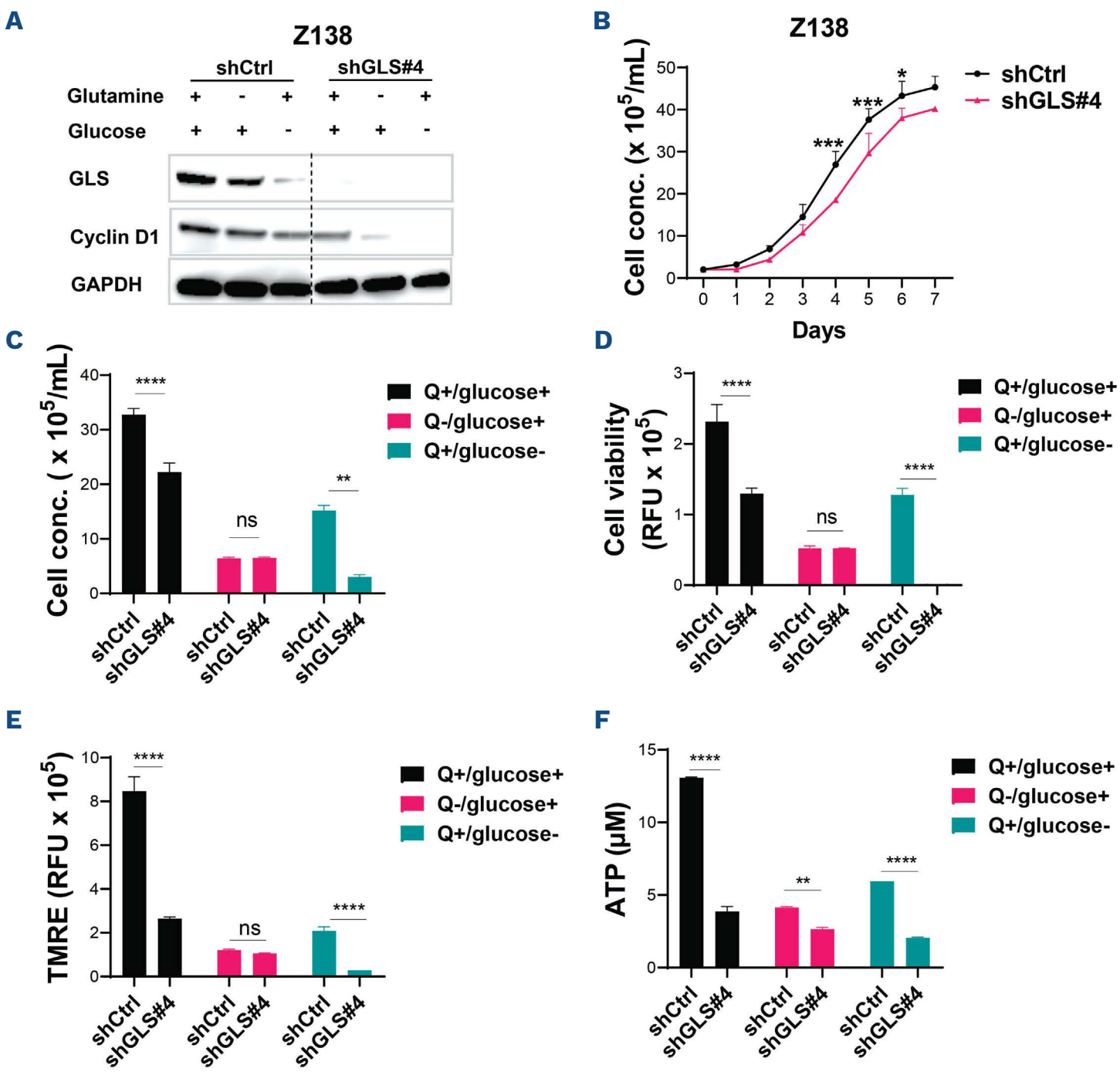

Figure 4. Glutaminase-mediated glutamine dependency promotes cell growth in ibrutinib-resistant cells. (A) Z138-shCtrl or Z138-shGLS#4 cells were cultured in medium with or without depletion of glutamine or glucose for 24 h and harvested for immunoblotting with the indicated antibodies. The dotted line indicates that the data were from different parts of the same gels. (B) Z138-shCtrl or Z138-shGLS#4 cells were cultured for 7 days and the cell titers were monitored. (C-F) Z138-shCtrl or Z138-shGLS#4 cells were seeded in complete medium containing glutamine and glucose (Q+/glucose+), or media deprived of glutamine (Q-/glucose+) or glucose (Q+/glucose-) and cultured for 24 h before proceeding with cell number counting (C), a cell viability assay (D), tetramethylrhodamine ethyl ester assay for mitochondrial membrane potential (E), or ATP generation assay (F). Two-way analysis of variance was used to determine statistical significance. ns: not significant; **P*<0.05; ***P*<0.01; ****P*<0.001; *****P*<0.0001. GLS: glutaminase; Q: glutamine; TMRE: tetramethylrhodamine ethyl ester; RFU: relative fluorescence units.

Z138-shCtrl cells (Figure 4E), while Z138-shGLS#4 cells showed a further loss of mitochondrial potential in response to glucose depletion but not glutamine depletion. Moreover, glutamine-dependent ATP production was greatly decreased by GLS knockdown (Figure 4F). Together, these data demonstrate that GLS-mediated glutamine dependency correlates with cell growth and ATP production in ibrutinib-resistant MCL cells. The data support our hypothesis that targeting GLS has the therapeutic potential to overcome ibrutinib resistance in MCL.

Glutaminase inhibition suppresses glutaminolysis and cell growth in mantle cell lymphoma cells.

Multiple GLS inhibitors are under clinical investigation for a broad range of solid tumors but not yet for MCL. These inhibitors include telaglenastat (CB-839), a specific, first-in-class GLS inhibitor that is in multiple clinical trials in

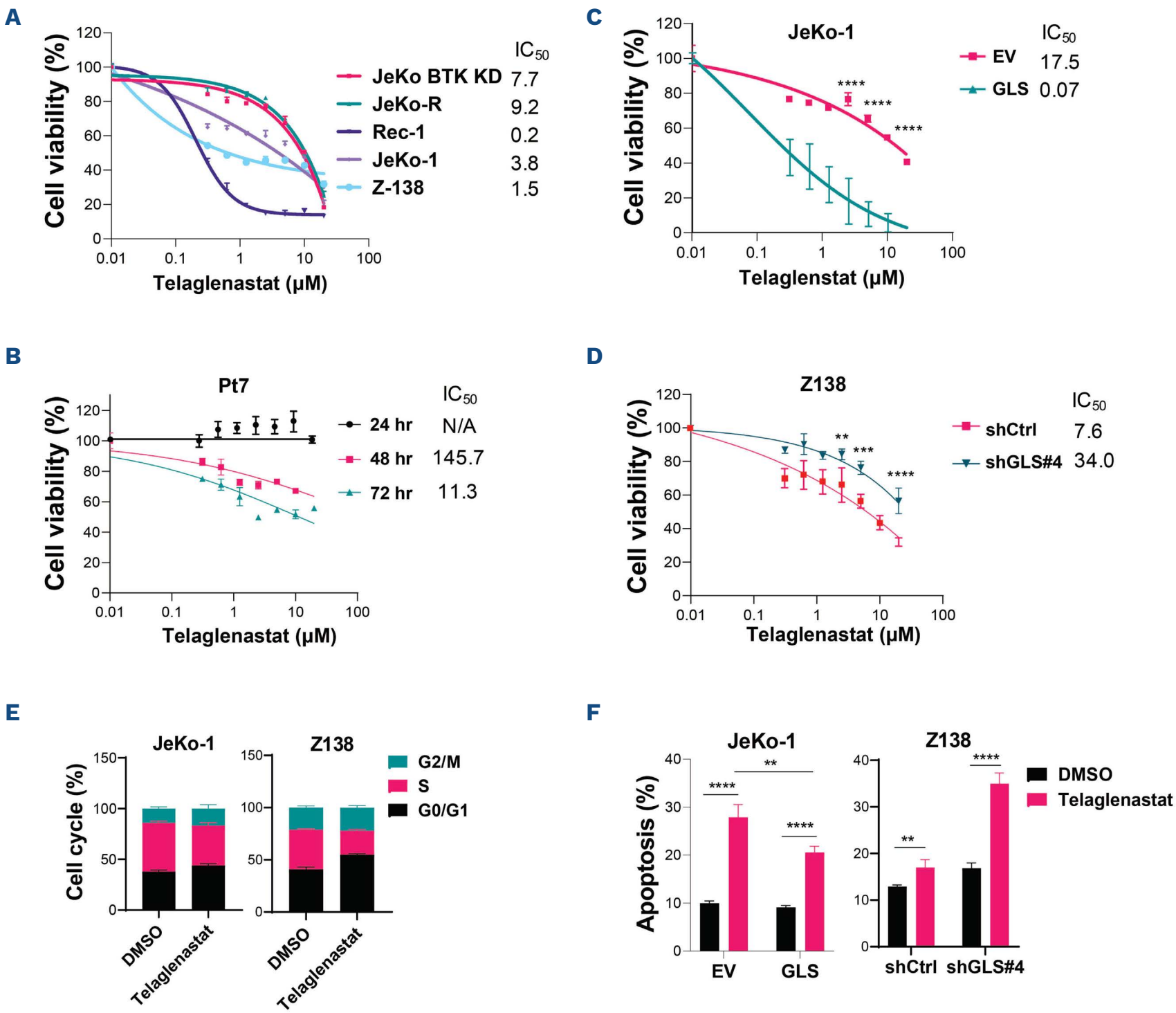

Figure 5. The glutaminase inhibitor telaglenastat suppresses growth of mantle cell lymphoma cells *in vitro* and *in vivo*. (A) Mantle cell lymphoma (MCL) cell lines were treated with telaglenastat at a 2-fold serial dilution from 20 μM and cell viability was determined at 72 h after treatment. The half maximal inhibitory concentration (IC_{50}) values were calculated and are shown on the right. (B) A patient's sample (Pt7) was treated with telaglenastat and cell viability was determined at the indicated time. The IC_{50} values were calculated as shown on the right. (C) JeKo-1 cells with or without stable glutaminase (GLS) overexpression (JeKo-1 EV and JeKo-1 GLS, respectively) were treated with telaglenastat at a 2-fold serial dilution from 20 μM and cell viability was determined at 72 h after treatment. (D) Z138-shCtrl and shGLS#4 cells were treated with telaglenastat at a 2-fold serial dilution from 20 μM and cell viability was determined at 72 h after treatment. (E) JeKo-1 or Z138 cells were treated with telaglenastat and cell cycle status was determined at 24 h after treatment. (F) JeKo-1 EV and JeKo-1 GLS and Z138 cells with or without GLS knockdown (Z138-shCtrl and Z138-shGLS#4) were treated with dimethylsulfoxide or 10 μM or 2 μM telaglenastat, respectively. The status of apoptosis was determined at 24 h after treatment. ***P*<0.01; ****P*<0.001; *****P*<0.0001. EV: empty vector; GLS: glutaminase; n/a: not available; DMSO: dimethylsulfoxide.

combination with other regimens. We therefore chose telaglenastat to inhibit GLS in MCL cells in this study. Telaglenastat effectively inhibited the proliferation of MCL cell lines with an IC_{50} of 0.22-9.2 μM (Figure 5A) and patients' MCL cells with an IC_{50} of 11.3 μM (Figure 5B) upon 72 hours of treatment. Telaglenastat showed greater efficacy in JeKo-1 cells with GLS overexpression than in the cells transduced with an empty vector control (Figure 5C). In line with this, Z138-shGLS#4 cells were more resistant than Z138-shCtrl cells to GLS inhibition (Figure 5D). Telaglenastat induced limited cell cycle arrest at the G0/G1 phase in JeKo-1 cells and more extensive arrest in Z138 cells (Figure 5E). Telaglenastat induced apoptosis in JeKo-1 EV cells but less in JeKo-1 cells with GLS overexpression (Figure 5F, left panel). Telaglenastat also induced apoptosis in Z138 with GLS knockdown but only slightly in Z138 control cells (Figure 5F, right panel). These data suggest that telaglenastat inhibits tumor cell growth primarily by blocking cell proliferation and not by inducing apoptosis in GLS-overexpressing cells. Indeed, telaglenastat treatment led to reduced expression of cell cycle-related proteins, including CDK4, cyclin D1, and cyclin B, in both JeKo-1 and Z138 cells (*Online Supplementary Figure S3C*). To assess the *in vivo* efficacy of GLS inhibition, we established a CDX model in immunodeficient NSG mice using Z138 cells. Telaglenastat treatment (200 mg/kg, orally, twice daily) significantly inhibited the growth of Z138 CDX tumors (P=0.004) and prolonged mouse survival (P=0.0017) (Figure 6A-C). As a systemic marker of tumor burden, serum β_2-microglobulin levels were also reduced in telaglenastat-treated mice compared to vehicle-treated ones (Figure 6D). Flow cytometry analysis using the tumor-specific cell surface markers CD20 and CD5 confirmed the tumor cell growth in each CDX tumor (*Online Supplementary Figure S4A, B*). Expression of Ki67 was markedly suppressed by telaglenastat treatment *in vivo*,

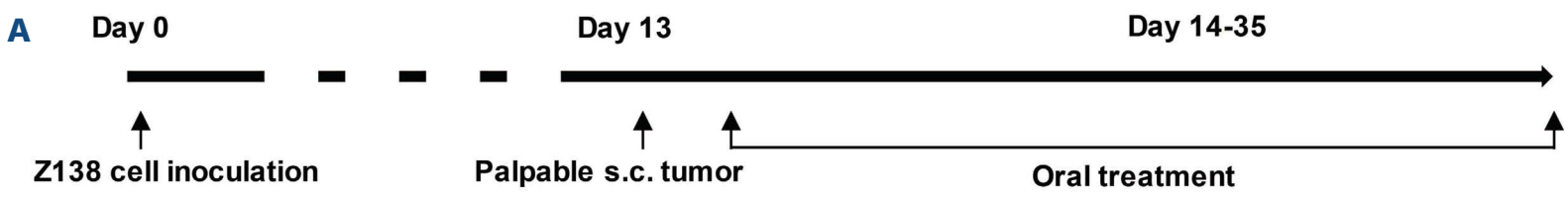

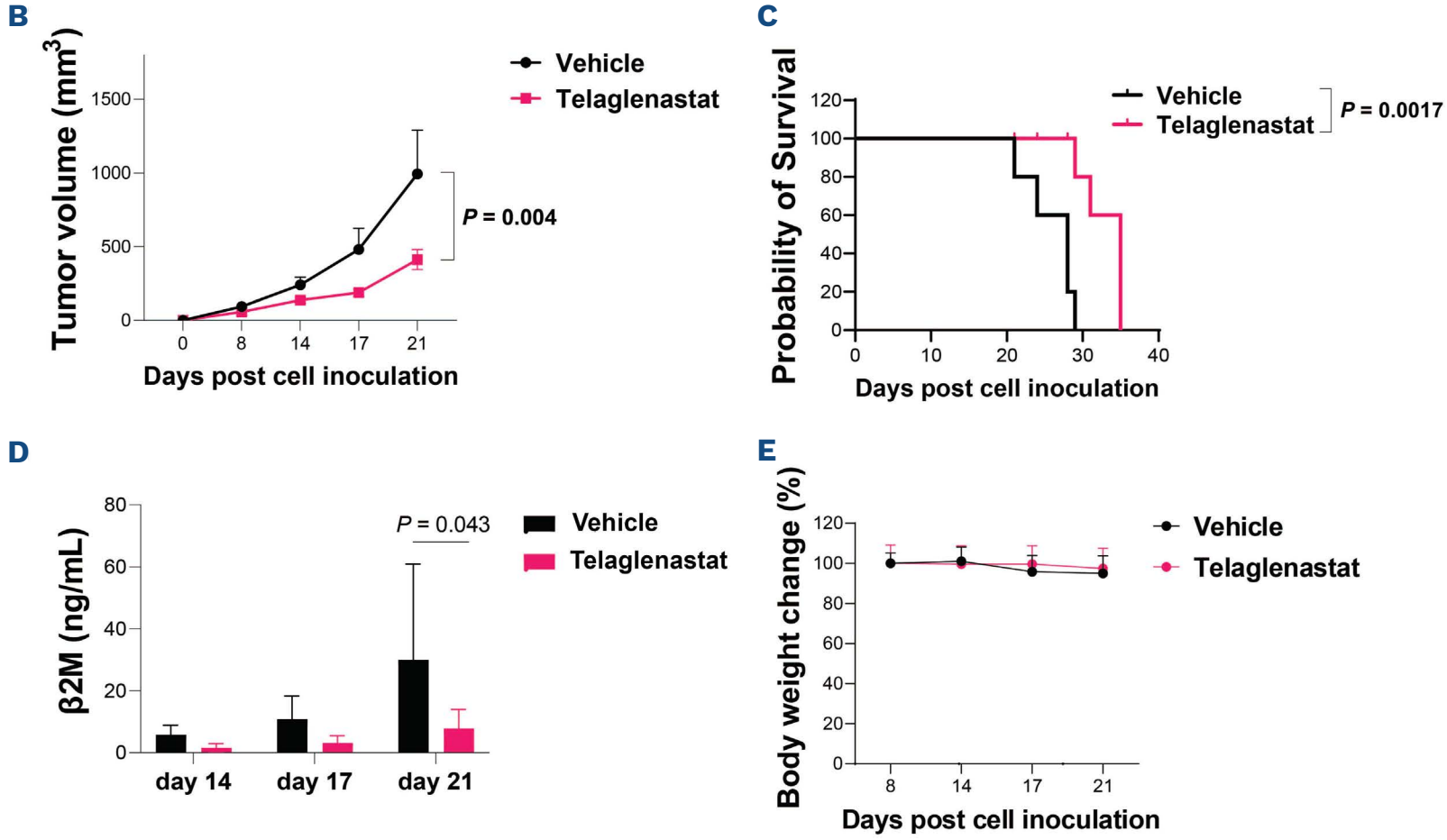

Figure 6. The glutaminase inhibitor telaglenastat suppresses cell growth of Z138 cells *in vivo*. (A) *In vivo* scheme of Z138 subcutaneous xenografts treated with vehicle or telaglenastat (200 mg/kg, twice/day) orally. (B) Tumor volume was documented at the indicated time points, with statistical significance of differences calculated at the endpoint. (C) A Kaplan-Meier plot for mouse survival was generated based on mouse survival after tumor inoculation. (D) Serum β_2-microglobulin levels were determined by enzyme-linked immunosorbent assay at the indicated time points. (E) Mouse body weight was monitored along with the treatments and percentage of body weight change relative to day 8 is shown. Two-way analysis of variance was used to determine statistical significance. ns: not significant; **P<0.01; ***P<0.001; ****P<0.0001. s.c.: subcutaneous; B2M: β_2-microglobulin.

when compared to that of vehicle-treated controls (*Online Supplementary Figure S4C*). No gross abnormalities were observed in the telaglenastat-treated mice, and there was no change in body weight (Figure 6E). These data demonstrate that targeting GLS by telaglenastat can effectively and safely inhibit the growth of Z138 CDX tumors and overcome ibrutinib resistance *in vivo*.

Telaglenastat improves the efficacy of ibrutinib or venetoclax *in vitro* and *in vivo*

Based on our data and previous studies,[22] telaglenastat acts primarily by inhibiting cell proliferation and not by inducing apoptosis. The aim of combination therapy in cancer treatment is to prevent the occurrence of resistance by acting synergistically.[23] We hoped that a combination of the cell proliferation blocker telaglenastat with clinically proven inducers of apoptosis, such as ibrutinib (a BTK inhibitor) and venetoclax (a BCL-2 inhibitor), might be synergistic. Indeed, we observed anti-MCL synergy in all MCL cell lines exposed to either telaglenastat plus ibrutinib or telaglenastat plus venetoclax (Figure 7A, B, *Online Supplementary Figure S5A, B* and *Online Supplementary Table S2*). Consistent with this, anti-MCL synergy was observed in the primary cells from a patient with MCL and two MCL PDX models (*Online Supplementary Figure S7C, D*, *Online Supplementary Table S2*). No apparent toxicity was observed for telaglenastat in peripheral blood mononuclear cells from a healthy donor (*Online Supplementary Figure S5C, D*), indicating that the dose range used (0-30 μM) does not cause off-target effects in

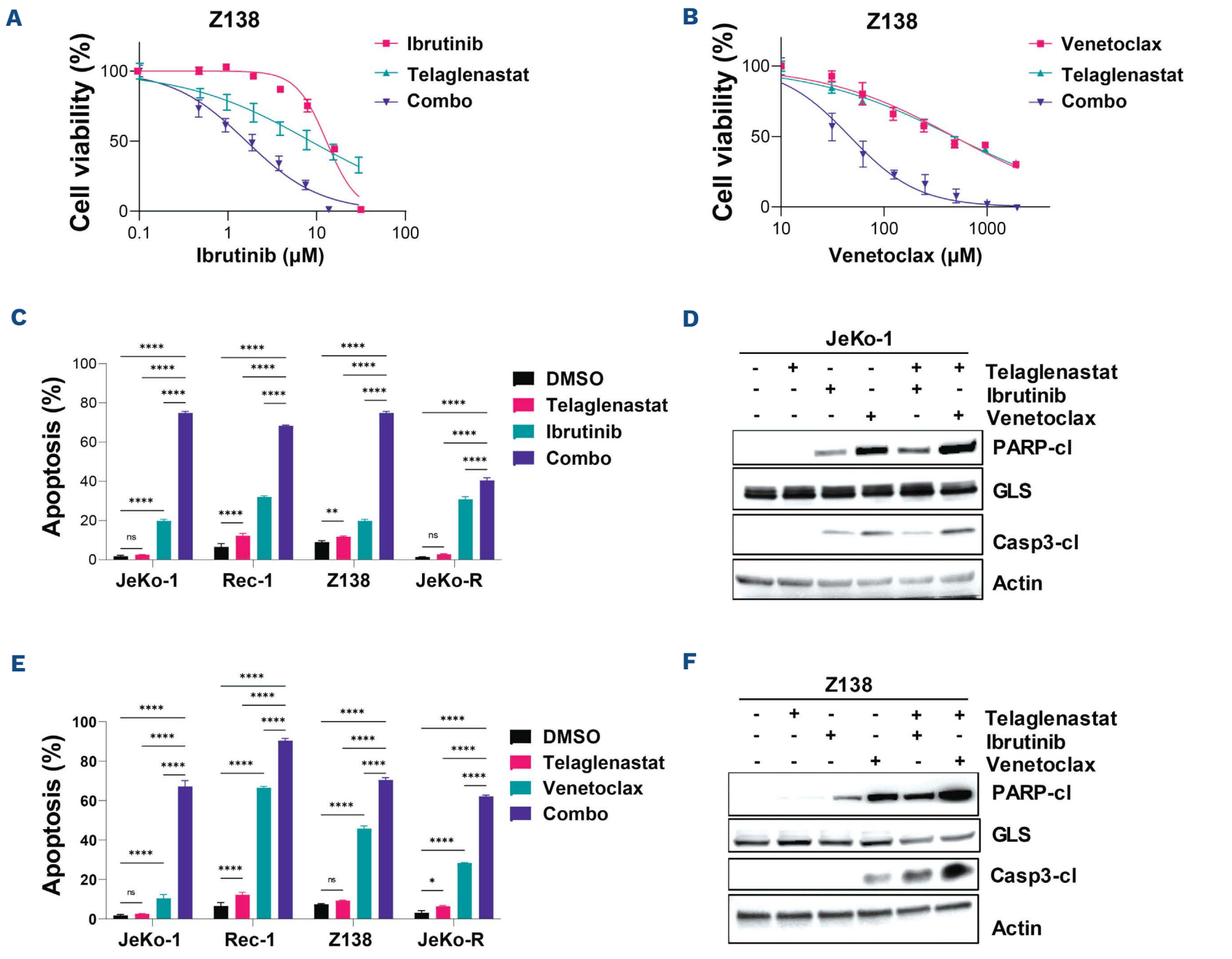

Figure 7. Telaglenastat shows synergistic anti-mantle cell lymphoma activity in combination with ibrutinib or venetoclax *in vitro*. (A, B) Cell viability was determined in Z138 cells treated with telaglenastat alone or in combination with ibrutinib (A) or venetoclax (B) for 72 h. The 2-fold serial dilutions of ibrutinib (A) and venetoclax (B) are indicated on the x-axis. The 2-fold serial dilutions of telaglenastat (0-20 μM) were used alone or in combination with ibrutinib or venetoclax, but are not indicated on the x-axis. (C-F) JeKo-1 and Z138 cells were treated with telaglenastat alone or in combination with ibrutinib (C, D) or venetoclax (E, F) for 24 h. The cells were harvested for assessment of apoptosis status by flow cytometry (C, E) and for immunoblotting using the indicated antibodies (D, F). Two-way analysis of variance was used to determine statistical significance. ns: not significant; **P*<0.05; ***P*<0.01; *****P*<0.0001. Combo: combination treatment; DMSO: dimethylsulfoxide; GLS: glutaminase.

healthy cells. The combinations of telaglenastat plus ibrutinib (Figure 7C), and telaglenastat plus venetoclax (Figure 7E) both showed potent synergy in inducing apoptosis, which was further validated by immunoblotting showing increased cleavage of caspase 3 and PARP (Figure 7D, F). Together, these data show the synergy between the clinically safe and potent drugs ibrutinib or venetoclax in combination with telaglenastat in MCL cells.

To further establish the clinical relevance of our findings, we took advantage of the previously established PDX-2 mouse model to investigate the combined effects of the drugs *in vivo* (*Online Supplementary Figure 6A*). The PDX-2 cells were not completely resistant to either ibrutinib or venetoclax when tested *in vitro* for 24 hours, suggesting that there is a window for improving efficacy. We hypothesized that targeting GLS might augment the efficacy of ibrutinib or venetoclax in the PDX, which did indeed show partial sensitivity to ibrutinib or venetoclax (Figure 8A, B). Both telaglenastat plus ibrutinib (Figure 8A, C), and telaglenastat plus venetoclax (Figure 8B, D) showed improved efficacy beyond that of single agents. This was further confirmed by serum β_2-microglobulin levels at day 86, an

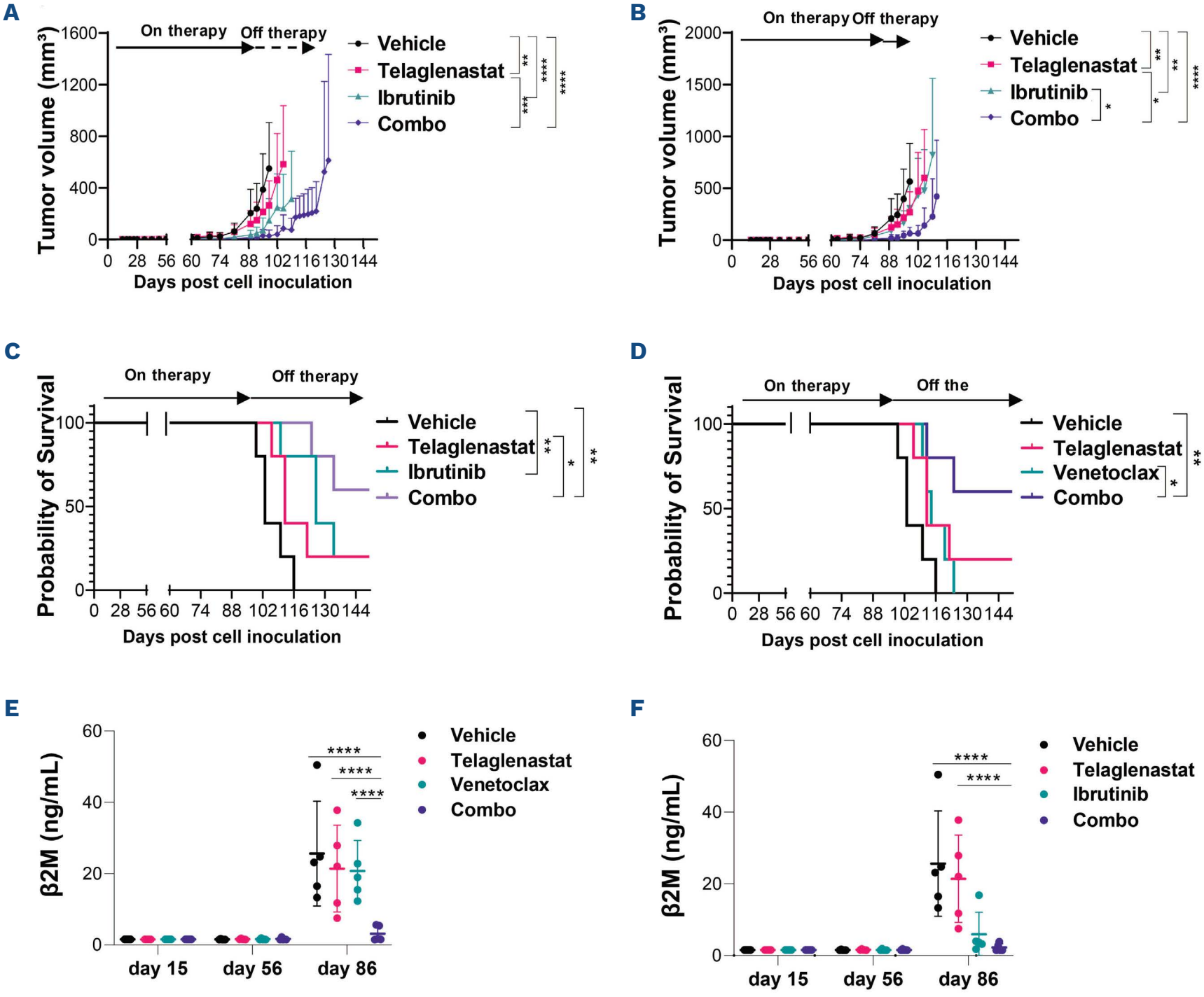

Figure 8. Telaglenastat in combination with ibrutinib or venetoclax shows synergistic anti-mantle cell lymphoma activity in a patient-derived xenograft model. PDX-2 subcutaneous xenografts were established in NSG mice. The mice were randomly grouped and treated orally with vehicle (daily), telaglenastat (100 mg/kg, twice daily), ibrutinib (50 mg/kg, daily), venetoclax (10 mg/kg, daily) or combinations of drugs at day 56 after cell inoculation. (A, B) Tumor volume at the indicated time-points, with the statistical significance of differences calculated at the endpoint when the first mouse in the treatment group reached the limit of tumor size. (C, D) Kaplan-Meier plots were generated based on the survival time of each individual mouse. (E, F) Serum β_2-microglobulin levels were determined by enzyme-linked immunosorbent assay at day 15 (pre-treatment), day 56 (start of treatment) and day 86 (after 30 days on treatment), before the tumors in all mice carrying the patient-derived xenograft model became measurable. Two-way analysis of variance was used to determine statistical significance. ns: not significant; **P*<0.05; ***P*<0.01; *****P*<0.0001. Combo: combination treatment; B2M: β_2-microglobulin.

early time-point of tumor growth before the tumors in all mice carrying the PDX model became measurable (Figure 8E, F). Again, we confirmed that the percentages of MCL cells present in the tumors were comparable across the treatment groups (*Online Supplementary Figure S6B-D*), and no gross abnormalities were observed in mice treated with any of the single agents or combinations (*Online Supplementary Figure S6E, F*). Taken together, these findings demonstrated improved efficacy of the two combinations tested in MCL cells, both *in vitro* and *in vivo*, paving the way for future clinical investigation of telaglenastat drug combination strategies in MCL.

Discussion

For the many types of cancer relying on glutaminolysis for energy metabolism to support rapid tumor growth,[24] targeting glutaminolysis is a plausible therapeutic strategy. To examine this possibility, we determined the role of GLS in ibrutinib resistance and assessed the potential of targeting GLS alone or in combination with either ibrutinib or venetoclax in preclinical MCL models. We confirmed that GLS expression was upregulated in ibrutinib-resistant MCL cells and associated with a poor clinical outcome. The cancer hallmark MYC_TARGETs_v1 was the predominant signaling pathway associated with ibrutinib-resistance in MCL patients.[3] The proto-oncogene MYC promotes glutaminolysis and glutamine dependency by inducing expression of the major glutamine transporters ASCT2 and SN2 and the enzyme GLS, which is responsible for the first catalytic event of glutaminolysis. In this study, we confirmed that the expression of both GLS and ASCT2 was associated with glutaminolysis in MCL. Blocking glutamine uptake with the ASCT2-specific inhibitor V-9302 led to marked reduction of both GLS expression and MYC expression. MYC knockdown resulted in reduced GLS and ASCT2, while MYC overexpression promoted their expression. Therefore, glutamine dependency in ibrutinib-resistant MCL cells is likely due to a positive feedback loop of MYC-ASCT2-GLS-glutaminolysis (*Online Supplementary Figure S7*). It will be interesting to investigate whether this positive feedback loop in contributing to therapeutic resistance to BTK inhibitors also applies to other types of non-Hodgkin lymphoma with MYC overexpression, such as diffuse large B-cell lymphoma.

Depleting GLS from formerly GLS-overexpressing cells led to release from glutamine dependency and a switch to greater dependency on glycolysis. Conversely, GLS ectopic overexpression resulted in enhanced glutamine dependency for tumor cell growth. Therefore, GLS overexpression promotes glutaminolysis. GLS depletion did not affect cell survival, but greatly affected mitochondrial membrane potential, ATP production, and cell growth. Consistent with this, GLS inhibition by telaglenastat in cells with high GLS expression did not cause marked cell death, but significantly slowed cell growth. However, we observed strong synergy in inducing cell death when telaglenastat was combined with the potent apoptosis inducers ibrutinib or venetoclax. It is possible that targeting GLS to turn off glutaminolysis-dependent cellular energy metabolism may prime cells expressing high levels of GLS to be more sensitive to agents such as ibrutinib and venetoclax, which potently induce apoptosis. Therefore, GLS is a therapeutic target for MCL cells with glutamine dependency, and GLS inhibition-based combination treatment will act synergistically to induce tumor vulnerability. A synergistic anti-tumor activity of telaglenastat in combination with venetoclax has also been seen in acute myeloid leukemia.[25] It is, therefore, possible that a combination of a GLS inhibitor with other agents used in the treatment of non-Hodgkin lymphomas, such as cytotoxic agents, could also augment the efficacy of therapy beyond that of the single agents, although this requires further investigation.

This is the first study dissecting the role of GLS in glutamine dependency associated with ibrutinib resistance in MCL and targeting glutaminolysis using the clinically investigated GLS inhibitor telaglenastat in MCL cells. Telaglenastat is currently under multiple clinical investigations in combination with other regimens to enhance the clinical efficacy over that of single agents. Our study provides preclinical evidence supporting the combination approach in targeting GLS and other vulnerabilities in treating MCL.

Disclosures

MW has received research support from Acerta Pharma, AstraZeneca, BeiGene, BioInvent, Celgene, Genmab, Genentech, Innocare, Janssen, Juno Therapeutics, Kite Pharma, Lilly, Loxo Oncology, Molecular Templates, Oncternal, Pharmacyclics, VelosBio, and Vincerx; has received speaker's honoraria from Acerta Pharma, Anticancer Association, AstraZeneca, BeiGene, BGICS, BioInvent, CAHON, Clinical Care Options, Dava Oncology, Eastern Virginia Medical School, Epizyme, Hebei Cancer Prevention Federation, Imedex, Janssen, Kite Pharma, Leukemia and Lymphoma Society, LLC TS Oncology, Medscape, Meeting Minds Experts, Miltenyi Biomedicine GmbH, Moffit Cancer Center, Mumbai Hematology Group, OMI, OncLive, Pharmacyclics, Physicians Education Resources (PER), Practice Point Communications (PPC), and The First Afflicted Hospital of Zhejiang University; and is a consultant to AstraZeneca, BeiGene, CSTone, Deciphera, DTRM Biopharma (Cayman) Limited, Epizyme, Genentech, InnoCare, Janssen, Juno Therapeutics, Kite Pharma, Lilly, Loxo Oncology, Miltenyi Biomedicine GmbH, Oncternal, Pharmacyclics, and VelosBio. The other authors have no conflicts of interest to disclose.

Contributions

MW, VCJ, YY, and LL conceived the study; LL, VCJ, and YY designed it; VCJ, LN, and YY supervised the study. LL, LN, QC, AJ, YL, YJL, YC, JV, ZC, AL, and WW acquired the data; LL, VCJ, LN, and YY analyzed and interpreted the data. LL wrote the original draft of the manuscript; VCJ and LN reviewed and edited the manuscript; MW acquired funding for the study.

Acknowledgments

The authors would like to thank the patients and their families who contributed to this research study and Paul Dolber for critical editing of the manuscript.

Funding

This study was supported by various philanthropic donors.

Data-sharing statement

The RNA sequencing dataset reported in our previous study has been deposited in the European Genome-Phenome Archive (EGA) database and the access number is EGAS00001003418. Other original data are available from the corresponding author on reasonable request.

References

1. Jain P, Dreyling M, Seymour JF, Wang M. High-risk mantle cell lymphoma: definition, current challenges, and management. J Clin Oncol. 2020;38(36):4302-4316.
2. Wang ML, Rule S, Martin P, et al. Targeting BTK with ibrutinib in relapsed or refractory mantle-cell lymphoma. N Engl J Med. 2013;369(6):507-516.
3. Zhang L, Yao Y, Zhang S, et al. Metabolic reprogramming toward oxidative phosphorylation identifies a therapeutic target for mantle cell lymphoma. Sci Transl Med. 2019;11(491):eaau1167.
4. Duraj T, Carrion-Navarro J, Seyfried TN, Garcia-Romero N, Ayuso-Sacido A. Metabolic therapy and bioenergetic analysis: the missing piece of the puzzle. Mol Metab. 2021;54:101389.
5. Samudio I, Fiegl M, Andreeff M. Mitochondrial uncoupling and the Warburg effect: molecular basis for the reprogramming of cancer cell metabolism. Cancer Res. 2009;69(6):2163-2166.
6. Bolzoni M, Chiu M, Accardi F, et al. Dependence on glutamine uptake and glutamine addiction characterize myeloma cells: a new attractive target. Blood. 2016;128(5):667-679.
7. Patel D, Menon D, Bernfeld E, et al. Aspartate rescues S-phase arrest caused by suppression of glutamine utilization in KRas-driven cancer cells. J Biol Chem. 2016;291(17):9322-9329.
8. Márquez J, Campos-Sandoval JA, Peñalver A, et al. Glutamate and brain glutaminases in drug addiction. Neurochem Res. 2017;42(3):846-857.
9. Guo H, Zeng D, Zhang H, et al. Dual inhibition of PI3K signaling and histone deacetylation halts proliferation and induces lethality in mantle cell lymphoma. Oncogene. 2019;38(11):1802-1814.
10. Li CJ, Jiang C, Liu Y, et al. Pleiotropic action of novel Bruton's tyrosine kinase inhibitor BGB-3111 in mantle cell lymphoma. Mol Cancer Ther. 2019;18(2):267-277.
11. Zhang S, Jiang VC, Han G, et al. Longitudinal single-cell profiling reveals molecular heterogeneity and tumor-immune evolution in refractory mantle cell lymphoma. Nat Commun. 2021;12(1):2877.
12. Jiang C, Zhu Y, Zhou Z, et al. TMEM43/LUMA is a key signaling component mediating EGFR-induced NF-kappaB activation and tumor progression. Oncogene. 2017;36(20):2813-2823.
13. Dobin A, Davis CA, Schlesinger F, et al. STAR: ultrafast universal RNA-seq aligner. Bioinformatics. 2013;29(1):15-21.
14. Love MI, Huber W, Anders S. Moderated estimation of fold change and dispersion for RNA-seq data with DESeq2. Genome Biol. 2014;15(12):550.
15. Subramanian A, Tamayo P, Mootha VK, et al. Gene set enrichment analysis: a knowledge-based approach for interpreting genome-wide expression profiles. Proc Natl Acad Sci U S A. 2005;102(43):15545-15550.
16. Liberzon A, Birger C, Thorvaldsdottir H, Ghandi M, Mesirov JP, Tamayo P. The Molecular Signatures Database (MSigDB) hallmark gene set collection. Cell Syst. 2015;1(6):417-425.
17. Li JCA. Modeling survival data: extending the Cox model. Sociol Method Res. 2003;32(1):117-120.
18. Ren P, Yue M, Xiao D, et al. ATF4 and N-Myc coordinate glutamine metabolism in MYCN-amplified neuroblastoma cells through ASCT2 activation. J Pathol. 2015;235(1):90-100.
19. Gao P, Tchernyshyov I, Chang TC, et al. c-Myc suppression of miR-23a/b enhances mitochondrial glutaminase expression and glutamine metabolism. Nature. 2009;458(7239):762-765.
20. Vasan K, Clutter M, Dunne SF, et al. Genes involved in maintaining mitochondrial membrane potential upon electron transport chain disruption. Front Cell Dev Biol. 2022;10:781558.
21. Friday E, Oliver R, Welbourne T, Turturro F. Glutaminolysis and glycolysis regulation by troglitazone in breast cancer cells: relationship to mitochondrial membrane potential. J Cell Physiol. 2011;226(2):511-519.
22. Lee P, Malik D, Perkons N, et al. Targeting glutamine metabolism slows soft tissue sarcoma growth. Nat Commun. 2020;11(1):498.
23. Hanahan D, Bergers G, Bergsland E. Less is more, regularly: metronomic dosing of cytotoxic drugs can target tumor angiogenesis in mice. J Clin Invest. 2000;105(8):1045-1047.
24. Yang L, Venneti S, Nagrath D. Glutaminolysis: a hallmark of cancer metabolism. Annu Rev Biomed Eng. 2017;19:163-194.
25. Jacque N, Ronchetti AM, Larrue C, et al. Targeting glutaminolysis has antileukemic activity in acute myeloid leukemia and synergizes with BCL-2 inhibition. Blood. 2015;126(11):1346-1356.